

Half of the greenhouse gas emissions from China's food system occur during food production

Gang Liu ^{1,2}, Fan Zhang ^{1,2} & Xiangzheng Deng ^{1,2,3}✉

Food systems are responsible for a third of global anthropogenic greenhouse gas emissions and there has been an increasing research focus on food-system greenhouse gases. However, limited attention has been paid to emissions from the regional trade network associated with food systems. Here we developed a multi-regional input-output-based hybrid life cycle assessment model and traced China's food-system greenhouse gas emissions from farm to fork. China's food system emitted 2.4 (95%; confidence interval range: 1.6–3.2) gigatons CO₂-equivalent in 2019, and half were emitted at the production stage. There were substantial differences in the emission structure and sources among the provinces. Further analysis indicated that the differences among provinces were caused by the separation of food production and consumption. People living in wealthier coastal and central regions consumed food from western and northeastern regions. Therefore, the government should consider interregional synergies when developing strategies to reduce food-system greenhouse gas emissions.

¹Key Laboratory of Land Surface Pattern and Simulation, Institute of Geographic Sciences and Natural Resources Research, Chinese Academy of Sciences, Beijing, China. ²College of Resources and Environment, University of Chinese Academy of Sciences, Beijing, China. ³School of Economics and Management, University of Chinese Academy of Sciences, Beijing, China. ✉email: dengxz@reis.ac.cn

Global greenhouse gas (GHG) emissions have increased with the growth of industrialization and a series of climate problems such as global warming has emerged. The major component of anthropogenic GHGs—carbon dioxide (CO₂)—is usually regarded as the target for emission reduction and it is the focus of most policies and plans. Non-CO₂ GHGs, such as methane (CH₄) and nitrous oxide (N₂O), are capable of absorbing more heat with reference to the value of 100-year global warming potential (GWP100)¹. Reducing their emissions has the advantage of creating more climate benefits and lowering the overall cost of mitigation^{2–5}. Non-CO₂ GHG mitigation, therefore, plays a vital role of efficient climate mitigation strategies⁶. Establishing an overall GHG emission reduction system that takes into account all economic sectors require substantial time and technical inputs⁷. Setting emission reduction targets for different industries one at a time is the basis and starting point for formulating reduction measures covering all sectors in the future. Food systems, which contribute one-third of global anthropogenic GHG emissions, could be a priority for setting GHG reduction targets, especially for developing countries^{8,9}.

Greenhouse gases are released at every food-system life cycle stage: cultivation, capture or harvest, transportation, processing, packaging, consumption and disposal of food waste. The food system's operation also involves the consumption and conversion of energy. The material and energy required depend on the use of raw materials (such as fertilizer) that produce additional GHG emissions^{10–13}. In developing countries, the contributions of emissions associated with farm gate production is a dominant stage in food system emissions^{14–16}. A considerable amount of research has been conducted on GHG emissions from agriculture, covering various gases including CO₂^{17–19} and non-CO₂ (such as CH₄ and N₂O)^{20–22}. Recently, a growing body of literature has recognized that accounting for food-system GHG emissions using a systematic approach is an effective way to understand the mitigation potential of the system^{16,23–25}. In addition to food-system GHG emissions within a country or region, researchers also have shown an increased interest in the interregional transfer of food-system GHGs via the trade network, covering wide spatial and temporal scales^{26–28}. China, as one of the largest GHG emitters, lacks detailed knowledge of food-system GHG emissions, particularly when supply chains and regional trade networks are considered.

In this study, we developed a multi-regional input-output-based hybrid life cycle assessment (MIRO-based hybrid LCA) model with the aim of filling this gap using a comprehensive methodological framework. The LCA was able to identify and analyze the environmental factors and potential influences of food-system supply chains^{29–31}, while the MRIO is a useful tool for investigating the linkage among sectors and interregional trade^{32,33}. We explored the characteristics of national and provincial food systems in China to improve the understanding of emissions related to the production, transportation, consumption and waste throughout its different stages and sectors of China's food system. This study will help stakeholders better understand the components and sources of food-system GHG emissions, as well as provide opportunities for the mitigation of China's food-system GHGs.

Results

National food-system greenhouse gas emissions. Our estimate of the total GHG contribution of China's food system was 2.4 (95% CI range: 1.6–3.2) Gt CO₂-equivalent (CO₂e) in 2019 (Fig. 1). Carbon dioxide is the primary GHG induced by human activities and it is also the major component of food-system emissions. In 2019, approximately 1.2 (95% CI range: 0.7–1.6)

Gt CO₂e (47.6%) of emissions were attributed to CO₂, in line with FAOSTAT^{12,15}. From production to consumption, CO₂ escaped at each life cycle stage of the food system. The packaging stage, contributing 0.4 (95% CI range: 0.2–0.6) Gt CO₂e, was the leading source of CO₂ emissions, while CO₂ emissions from retail formed the smallest share. Previous studies have revealed similar findings^{12,15}.

China's food system emitted 0.8 (95% CI range: 0.4–1.3) Gt CO₂e of CH₄, which accounted for 34.1% of total emissions. The CH₄ emissions were mainly from the production and waste stages. The proportion of CH₄ in food-system GHG emissions was notable although CH₄ accounted for only 13.2% of China's anthropogenic GHG emissions in 2018 (expressed in CO₂e)³⁴. This discrepancy may be attributed to the substantial agriculture's contribution to CH₄ emissions, driven by livestock farming and rice paddies³⁵. We found that N₂O had the second lowest proportion of GHG emissions at only 14.1%, mainly owing to agricultural production. Although fuel combustion contributed to N₂O emissions, livestock manure management and fertilizer use in crop cultivation at the production stage were the major contributors. F-gases estimated to be responsible for only 4.2% of total emissions, with the majority escaping during the retail stage.

Half of China's food-system GHGs (50.2%) were emitted at the production stage. In 2019, China released 1.2 (95% CI range: 0.8–1.6) Gt CO₂e GHGs from food production, including 25.0% of CO₂, 52.5% of CH₄ and 22.5% of N₂O. Of the emissions from production, emissions from energy and non-energy activities account for 17.8% and 82.2% of total emissions, respectively. In contrast to other life cycle stages, the production, retail and waste stages had very high proportions of non-CO₂ GHGs, while CO₂ was the dominant GHG for other stages. The packaging stage was the most important contributor of CO₂ emissions for food system, releasing 0.4 (95% CI range: 0.2–0.6) Gt CO₂e of CO₂. The GHG emissions from the transport stage was the lowest, accounting for merely 5.4% of food-system emissions.

Regional food-system greenhouse gas emissions in China. To examine China's regional GHG emissions for the food system, we evaluated the provincial contributions, considering emissions for various gases and life cycle stages. As shown in Fig. 2, there was a notable discrepancy among the provinces for total GHG emissions. Inner Mongolia (Fig. 2, row 1, column 5) and Qinghai (Fig. 2, row 6, column 4) were the largest GHG emitter in China's food system, causing 128 (95% CI range: 83–173) Mt CO₂e and 127 (95% CI range: 87–167) Mt CO₂e of GHG emissions in 2019, respectively. GHG emissions from energy activities account for approximately 41.8% and 60.8% of GHG emissions in Inner Mongolia and Qinghai, respectively. Hunan (Fig. 2, row 3, column 6), Guangdong (Fig. 2, row 4, column 1) and Shandong (Fig. 2, row 3, column 3) were also important contributors, emitting 118 (95% CI range: 74–163) Mt CO₂e, 117 (95% CI range: 83–151) Mt CO₂e and 111 (95% CI range: 79–143) Mt CO₂e of GHGs, respectively. Only 28 (95% CI range: 19–37) Mt CO₂e of GHGs could be attributed to Tianjin (Fig. 2, row 1, column 2), which was the province with the lowest emissions. The emissions from Beijing (Fig. 2, row 1, column 1), Hainan (Fig. 2, row 4, column 3), and Shanghai (Fig. 2, row 2, column 3) were also low (39 (95% CI 26 to 52), 40 (95% CI 27 to 53) and 41 (95% CI 29 to 53) Mt CO₂e, respectively).

The components of the GHG emissions from food system varied greatly from province to province. Overall, CO₂, CH₄, N₂O and F-gases accounted for 47.6%, 34.1%, 14.1%, and 4.2% of the national food-system GHG emissions, respectively (Fig. 2). However, the share of different gases in provincial food-system GHG emissions differed from the national components. For

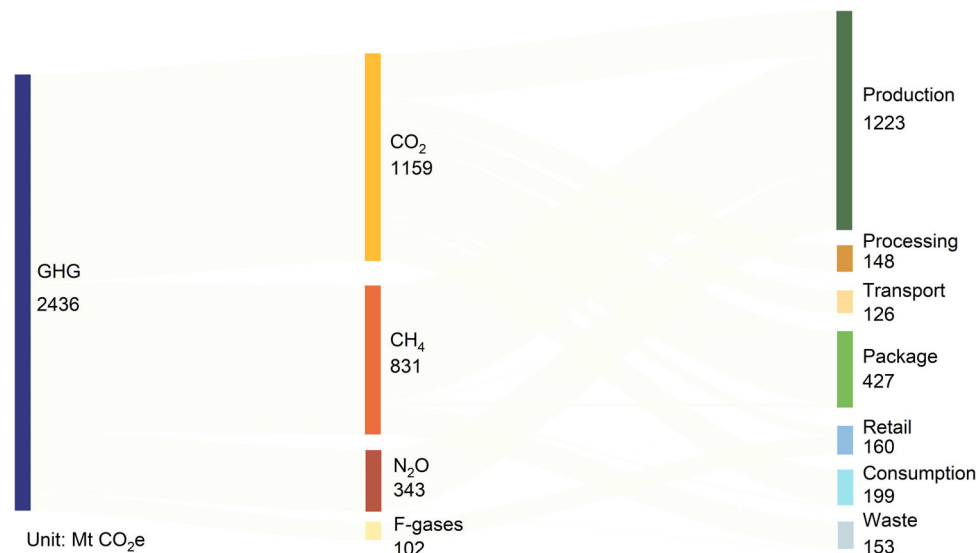


Fig. 1 China's food-system greenhouse gas (GHG) emissions. Total GHG (left bar), the contributions of different gases (bars in the middle) and the contributions of different life cycle stages (right bars). The numbers indicate the GHG in 2019 and are rounded. Emissions are expressed as CO₂e calculated using the values of the 100-year global warming potential (28 for CH₄ and 273 for N₂O). Because numbers are rounded, they do not necessary sum up to 100%.

example, CO₂ accounted for a very large proportion of food-system GHG emissions in Beijing (Fig. 2, row 1, column 1), Shanxi (Fig. 2, row 1, column 4) and Ningxia (Fig. 2, row 5, column 5). However, for Jiangxi (Fig. 2, row 3, column 2), Sichuan (Fig. 2, row 4, column 5) and Yunnan (Fig. 2, row 5, column 1), CH₄ took a larger share of food-system GHG emissions than CO₂. Furthermore, N₂O was responsible for a very small part of total food-system emissions in some provinces (e.g., less than 3% of the total emissions in Beijing) but made up a larger share in other provinces (e.g., 33.3% of Hainan's food-system GHG emissions). Similarly, the proportion of F-gases varies obviously across provinces.

Different life cycle stages of the food system had disparate contributions in various provinces, as seen in Fig. 2. Although the production stage contributed the most GHG emissions in China's food system, various stages of the life cycle were important in different provinces. For instance, the emissions from the production stage accounted for merely 8.4% of total food-system emissions in Beijing (Fig. 2, row 1, column 1), while the proportion of the production stage in the food system emissions of Sichuan (Fig. 2, row 4, column 5) was 67.0%. Furthermore, provinces with higher proportion of emissions at the production and waste stages typically had a larger share of CH₄, while provinces with higher share of the packaging stage in GHG emissions had a larger share of CO₂. For example, the total proportion of the production and waste stages in GHG emissions was 61.3% in Jiangxi (Fig. 2, row 3, column 2), with 51.8% of CH₄ emissions. For Beijing (Fig. 2, row 1, column 1), the GHG emission from packaging stage made up 38.7% and CH₄ contributed 17.5% of food-system emissions. A possible explanation for this might be that the types and proportions of GHGs from various food-system stages were different.

Contribution of non-CO₂ greenhouse gases to the food system.

Non-CO₂ GHGs were the vital contributors to China's food system as mentioned in section "National food-system greenhouse gas emissions". To compare the difference of non-CO₂ GHG contributions to food-system emissions among provinces, we evaluated the total non-CO₂ emissions, the portion of non-CO₂ gases in GHG emissions and the non-CO₂ emissions from

various sources. Figure 3a presented the spatial variation of food-system GHG emissions. It was reported that the provinces with the highest emissions were Heilongjiang Qinghai, Shandong, Henan, Hunan and Guangdong. The lowest GHG emissions were from Tianjin, Hainan, and Beijing at less than 40 Mt CO₂e. The three provinces with low GHG emissions all had a higher proportion of CO₂ emissions than that of CH₄ emissions. Among China's 30 provinces, four provinces (Tianjin, Ningxia, Shanghai and Hainan) had relatively small areas. This meant the land for agricultural production was limited, while the production stage was the main source of food-system emissions.

Figure 3b shows provincial non-CO₂ GHG emissions. By comparing Fig. 3a and Fig. 3b, it could be found that there were the synergies between total GHG emissions and non-CO₂ GHG emissions. In other words, for the provinces who having high total GHG emissions also tended to have higher non-CO₂ emissions. Therefore, non-CO₂ GHGs were the most important driver of food-system GHG emissions.

Figure 3c presents the non-CO₂ GHGs from different sources and the portion of non-CO₂ GHGs in provincial food-system. The non-CO₂ GHG sources varied obviously among different provinces. The non-CO₂ GHGs from production played a vital role in food-system non-CO₂ GHG emissions for the most provinces (e.g., Inner Mongolia, Hunan and Sichuan), while CH₄ from production had the relatively low contribution in other provinces (e.g., Beijing and Tianjin). The highest GHG emissions from waste management were in Guangdong—over 20 Mt CO₂e—while GHG emissions from waste management for the most provinces were less than 10 Mt CO₂e. Qinghai emitted the largest non-CO₂ GHG (8.8 Mt CO₂e) at the retail stage, followed by Gansu which released 7.3 Mt CO₂e of non-CO₂ gases at the retail stage. In three provinces (Beijing, Tianjin and Ningxia), the portion of non-CO₂ GHGs in food-system emissions was less than 0.3. Non-CO₂ GHGs for food system in Beijing accounted for only 0.27 of total GHG emissions.

Impacts of intraregional trade on China's greenhouse gas emissions from food system. The above results indicated that there were substantial differences among the provinces in the components and sources of GHG emissions. A recent global

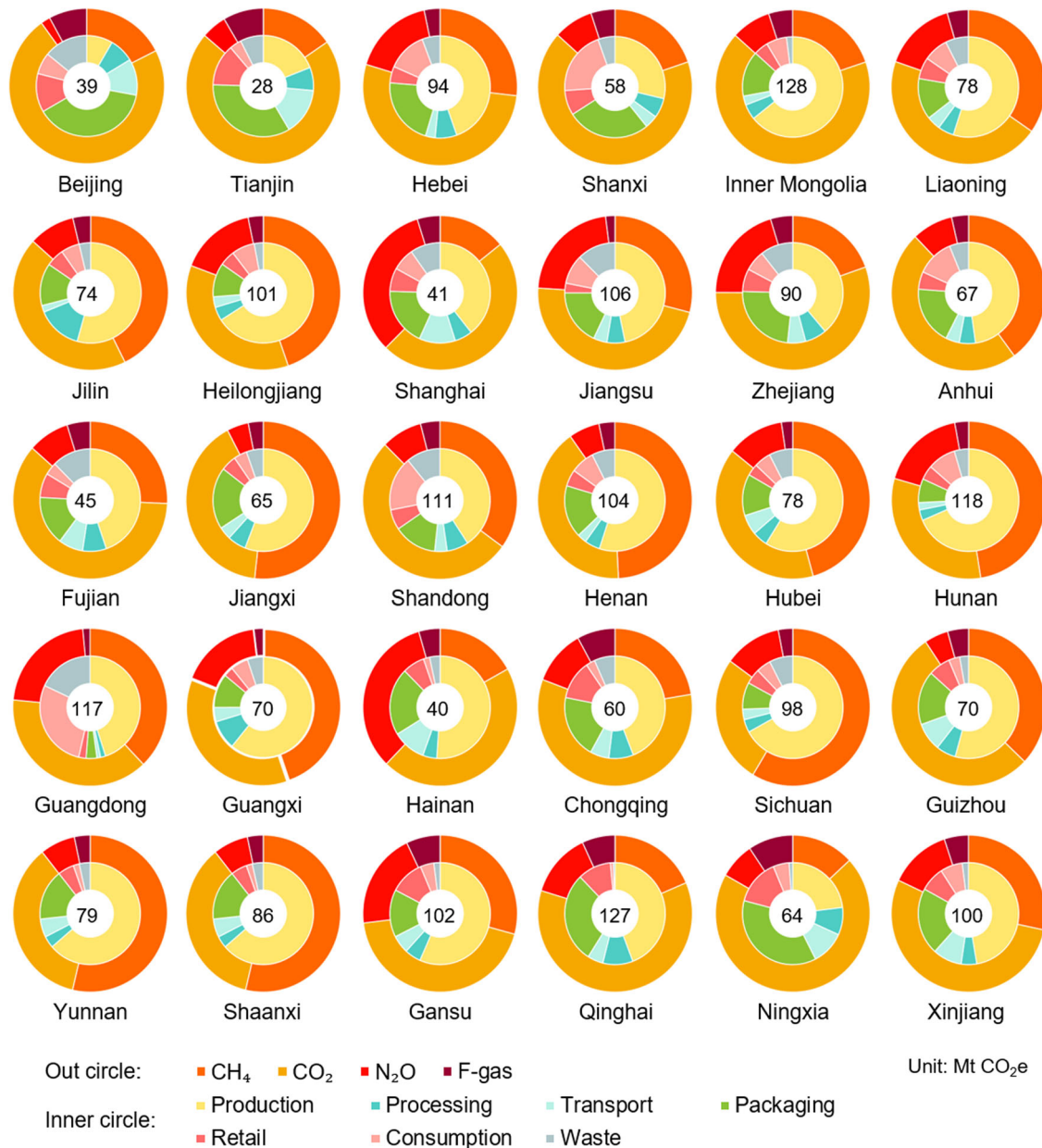


Fig. 2 Provincial food-system greenhouse gas emissions (GHGs) from various life cycle stages in 2019. Outer circles show the share of various greenhouse gas components, while inner circles express the proportion of each life cycle stage. Central numbers are the provincial total emissions. Because numbers are rounded, they do not necessary sum up to 100%.

analysis of food-production emissions revealed that approximately 22% of agricultural products were purchased in other regions from that where they were produced²⁸. It is possible, therefore, that the differences in China’s GHG emissions from food-system are related to interregional trade. In this section, we analyzed the regional discrepancy triggered by intraregional trade.

The total GHG emissions embodied in interregional trade were 0.7 (95% CI 0.5 to 0.9) CO₂e in 2019, which was 30.5% of China’s food-system emissions. Approximately 20.8% of embodied GHGs were attributed to intermediate input, while final consumption accounted for 79.2%. Intermediate input included agricultural products that went into other industries, such as food processing, whereas final consumption includes rural and urban consumption, government consumption, gross fixed capital formation, and stock increasing of agricultural products and food. Figure 4a, b illustrate the food-system GHG emissions transfer among the 30 provinces

via final consumption and intermediate input, respectively. For final consumption, the largest interregional transfer flow was from Gansu to Henan, with 13.7 Mt CO₂e of GHG emissions. Xinjiang exported total 48.5 Mt CO₂e of GHG emissions, which was the highest. Guangdong was the major importer for final consumption and 56.8 Mt CO₂e of GHG emissions transferred from other provinces to Guangdong. For intermediate input, the transferring is synergistic with final consumption.

Figure 4c shows the total trade in GHG emissions transferred among provinces, including final consumption and intermediate input. Guangdong had the largest volume of food-system GHG emission imports, with 73.9 Mt CO₂e. Henan ranked second with imports of 63.5 Mt CO₂e of GHG emissions. The province with the largest net imported volume of GHG emissions was Guangdong, with up to 59.2 Mt CO₂e. Xinjiang, located in northwest China, exported the largest volume of food-system GHG emissions in 2019, at 2.8 Mt CO₂e, followed by Qinghai,

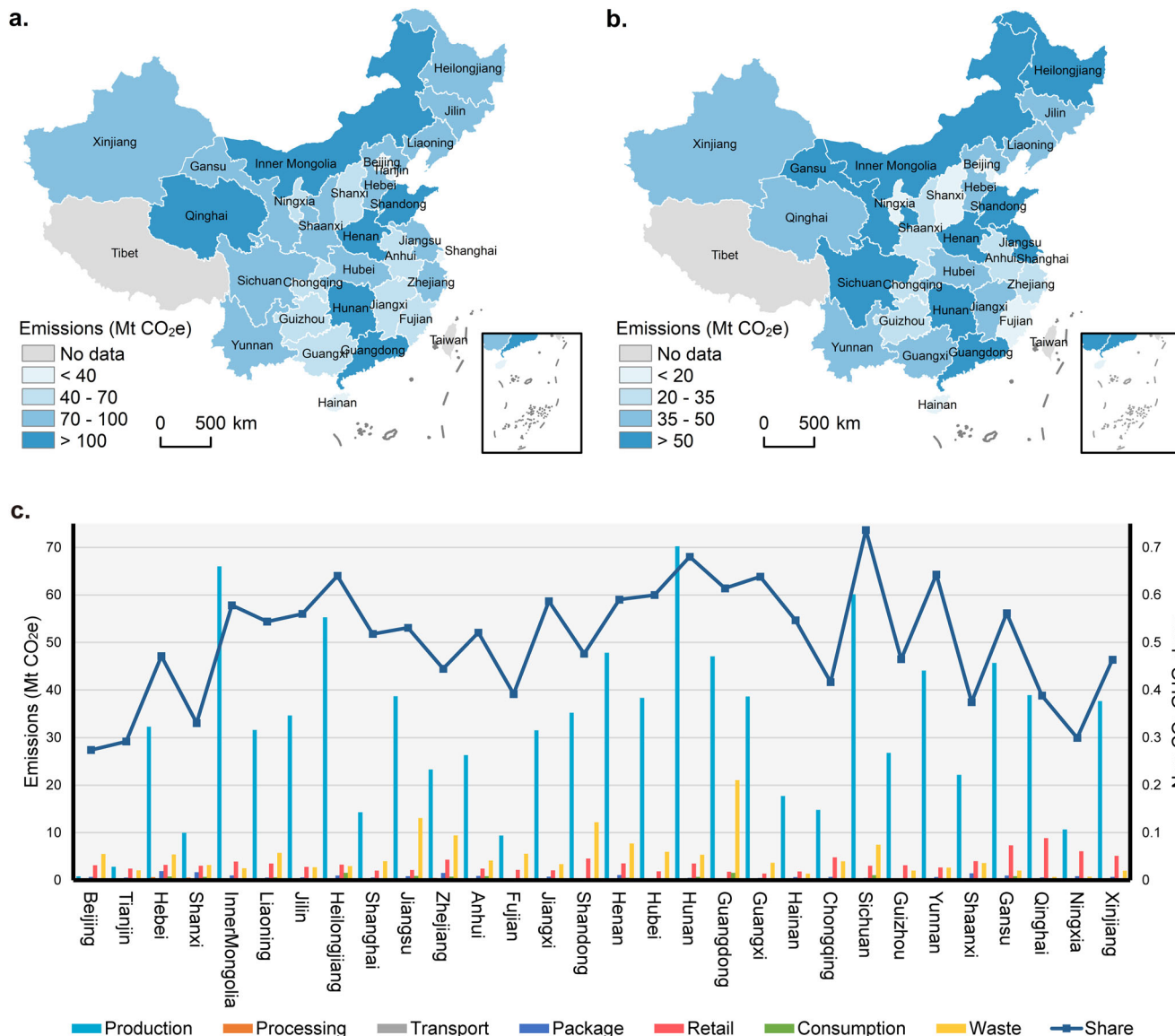


Fig. 3 Spatial differences in provincial greenhouse gas (GHG) emissions from food systems in 2019. **a** Total greenhouse gas emissions (drawing review No: GS (2016) 2929). **b** Non-CO₂ greenhouse gas emissions (drawing review No: GS (2016) 2929). **c** Contribution of different sources to non-CO₂ greenhouse gas. The base map in a, b was downloaded from the Resource and Environment Science and Data Center (<https://www.resdc.cn/DataList1.aspx?FieldTypeId=20,0>).

which had an export volume of 63.0 Mt CO₂e. Among the 30 provinces, the net trade flow of 12 provinces was negative and these provinces were net importers. In contrast, 18 provinces had a positive trade flow and these provinces were considered as net exporters.

Spatial characteristics of intraregional food-system greenhouse gas transfers. One interesting finding was that provinces with a net export of GHG emissions were generally located in the southwest and north of China, while provinces that imported GHG emissions were concentrated in the wealthier eastern and central China, as shown in Fig. 5a. For provinces with embodied GHG emissions exports, the proportions of non-CO₂ GHGs were larger than CO₂ and emissions from the production stage occupied a relatively large share (e.g., Gansu and Inner Mongolia). The proportion of GHG emissions from the waste and consumption stages was higher in provinces with embodied GHG emissions imports (e.g., Beijing and Zhejiang).

Figure 5b illustrates the dominating net trading flows of food-system embodied GHG among the eight regions. 30 provinces are grouped in to eight regions referring to previous work^{36,37}, and the details are shown in Supplementary Table S6. The Northeast, Northwest and Southwest of China were the main food-system GHG emission export regions and they were a vital guarantee of China’s food security. The Northwest region was an important part in the food-system GHG export, transferring a total of 230.3 Mt CO₂e of GHGs to Beijing–Tianjin, the North, Central, Central Coast, Southwest, and South Coast regions. The flow of food-system embodied GHGs from the Northwest to the Central regions was up to 91.2 Mt CO₂e. The South Coast was the major recipient of food-system embodied GHGs exported by the Southwest and it imported 28.6 Mt CO₂e of GHGs. In 2019, the Northeast exported 13.3 and 13.8 Mt CO₂e of GHGs via the interregional trade network to Central Coast and the North region, respectively. Another vital trade link was the flow from the Southwest region to the Central region, with 21.8 Mt CO₂e of GHGs. Therefore, the Southwest region was not only a recipient

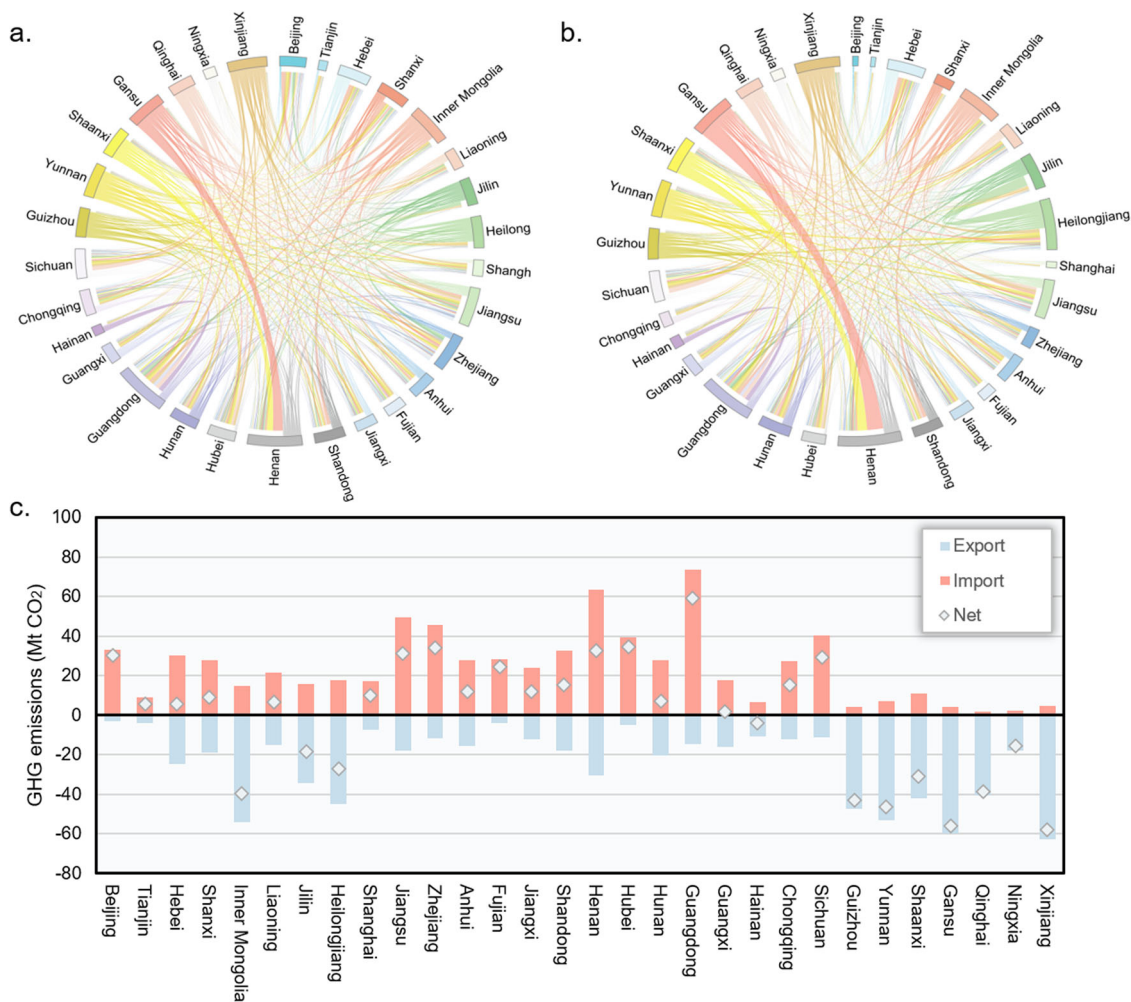


Fig. 4 Interregional transfers of food-system greenhouse gas emissions (GHG) along with the trade network among provinces. **a** Final consumption. **b** Intermediate input. **c** Sum of emissions transferred. For **a** and **b**, the width of ribbons denotes the volume of trading flow. The connection between provinces indicates the food-system GHG emissions transfer and the color of ribbons in line with the exporter. For **c**, positive numbers indicate imports, while negative numbers represent exports.

importing embodied GHG emissions from the Northwest, but it was also an exporter transferring GHGs to the Central. It was notable that Central Coast, which are regions with high population density and economic development, imported embodied GHGs from more than one region.

Discussion

Several estimate on China's food-system GHG emissions at the national level have been reported^{12,16}. These studies have mostly been global-scale estimates and have given specific emissions from China. China's food-system GHG emissions in 2018 estimated by Crippa et al.¹⁶ based on IPCC default emission factors are 2.5 Gt CO₂e, which are higher than our results, while FAO-STAT estimates for China's food-system total emission of 1.9 Gt CO₂e for 2019^{12,15}. In this study, our assessment suggests that the total GHG emissions from China's food system are 2.4 (95%; CI range: 1.6–3.2) Gt CO₂e, which is close to previous works within the overall uncertainty of these results. To adopt of various system boundaries and emission factors across studies is one of the primary reasons for the differences of reported figures. We adopted a bottom-up framework, where each province has independent emission factors rather than identical ones. And the emission factors for fuel chains³⁸ and domestic wastewater

emissions³⁹ refer to specialized studies, which are different to previous estimate on food-system emissions. This approach realized food-system emission estimates that are more in line with Chinese reality, but they are lower than that in the study of Crippa et al.¹⁶. Furthermore, our estimates for GHG emitted by energy system include the notable amounts of upstream emissions linked to the processing of fossil fuels, which possibly leads to the higher estimate than FAO-STAT^{12,15}. The estimate of Tubiello et al.¹² on China's food-system supply chain (stages except production) emissions in 2019 is 1.1 Gt CO₂e, while our estimate is 1.2 (95%; CI range: 0.9–1.5) Gt CO₂e which is consistent with existed finding.

Many efforts have also been made to conduct studies specifically targeting China's food production emissions^{40–43}. However, the majority of these studies cover only one or a few stages of the food system and are not on the basis of an integrated food system analysis framework. For instance, Zhang et al.⁴³ estimated emissions from the production and processing stages in China in 2017 as 1.6 Gt CO₂e, which is higher than our estimate. Crippa et al.¹⁶ estimates for the production and processing stages of 1.33 Gt CO₂e (in 2017 and 2018) are approximate to our findings. FAO-STAT reported the GHG emitted at production is 0.8 Gt CO₂e in 2019 accounting for 42% of total food-system emissions^{12,15}, which is in line with our estimate considering

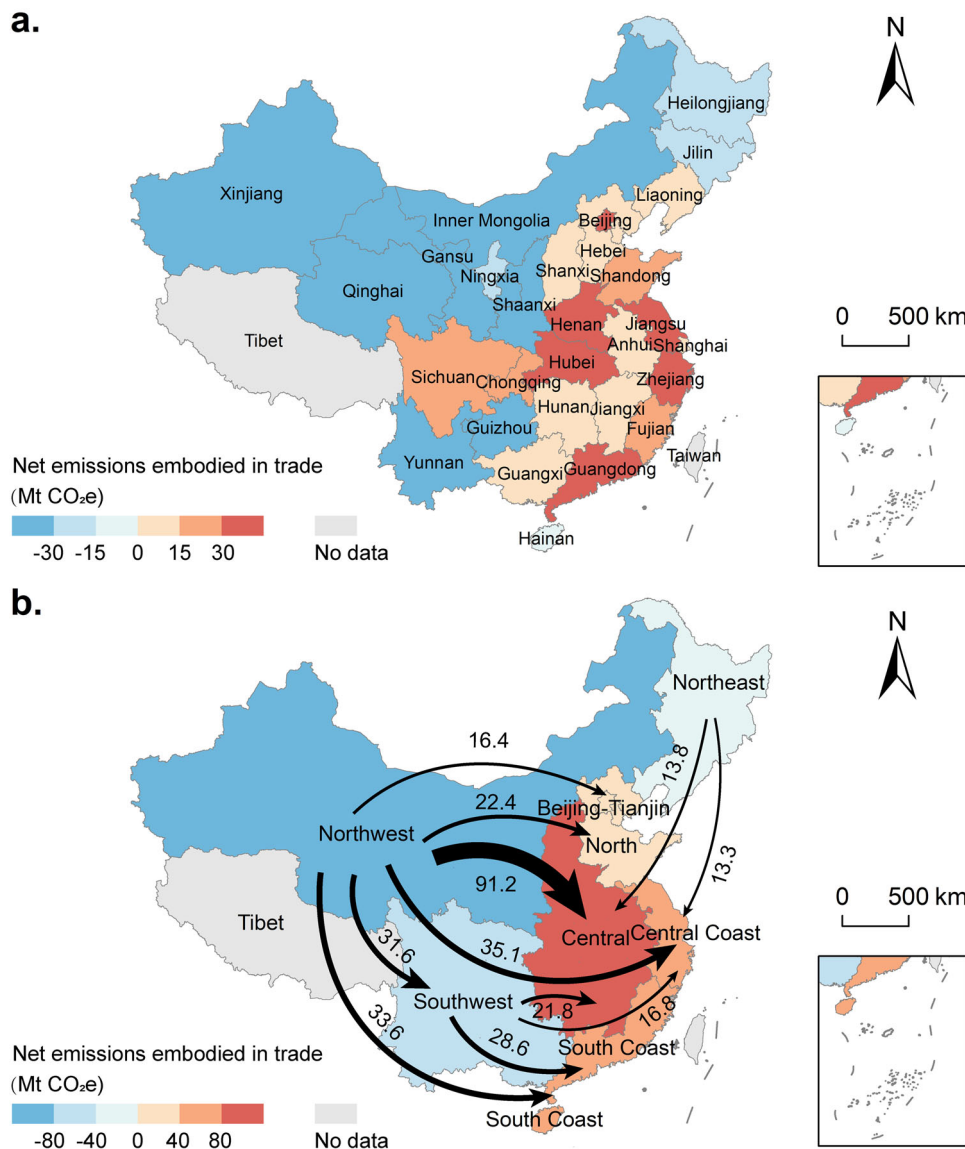


Fig. 5 Net greenhouse gas emissions embodied in trade. a Emissions embodied in trade among provinces. **b** Emissions embodied in trade regions. This study considered 30 provinces in China, excluding Tibet, Hong Kong, Macao, and Taiwan. The width of the black line indicates the net volume of emissions transfer. The base map in a, b was downloaded from the Resource and Environment Science and Data Center (<https://www.resdc.cn/DataList1.aspx?FieldTypeID=20,0>).

the underlying uncertainties. Due to the scarcity of similar studies, overall emissions of food system at the provincial level are incomparable. For GHG emissions transferring of China’s food system, discrepancy could be found in previous studies. On a global scale, intermediate trade and final consumption account for two-thirds and one-third of agricultural GHG emissions, respectively²⁶. If only agriculture is considered, the proportion of intermediate inputs and final consumption in this study is comparable to Zhao et al.²⁶. However, our research is based on an integrated food system perspective, with the food industry (which accounts for a larger share of final consumption) included in the accounting framework. Inconsistent results were obtained due to differences in accounting frameworks.

Beginning with the MRIO-based hybrid LCA based on provincial GHG emission inventory, our study evaluates the national and regional food-system emissions. GHG emissions from farm to fork are discussed, taking into account the intraregional trade. However, there are several limitations to our research. First, we do not account F-gases adopt from bottom to up owing to the

lack of necessary data. We used results from EDGAR-Food v6.0 and allocated national F-gases emissions to provinces based on energy consumption in each province during the retail stage. Then, MRIO tables are not updated on an annual basis. The 2017 MRIO table were used in this study, and this study ignored differences in the structure of the economy between 2017 and 2019. Besides, all production and consumption data in MRIO table is on the basis of currency, which is a common assumption in previous studies. Finally, our accounting framework only considers 30 Chinese provinces. Tibet, Hong Kong, Macau, and Taiwan are excluded due to a lack of data.

Conclusions

This study provided an analysis of China’s food-system GHG emissions covering each life cycle stage from production to waste and the embodied food-system GHG emissions transferred via the interregional trade network. At the national level, CO₂ was the dominant contributor, but the total share of non-CO₂ gases

was slightly more than half. The production stage emitted the largest proportion of food-system GHGs and was also one of the major sources of non-CO₂ GHGs. The provincial view was diverse, with remarkable differences in the composition and sources of food-system GHG emissions among the provinces.

Unlike the overall anthropogenic GHG emissions, the portion of non-CO₂ to the food-system was considerable. Despite non-CO₂ GHGs from various sources of food-system emissions differing among provinces, the synergies between total and non-CO₂ GHG emissions suggested that non-CO₂ GHGs were the important drivers of food-system GHG emissions. The production and waste stages were the two main contributors to non-CO₂ GHGs, while the packaging stage was the major source of CO₂. Considering the important contribution of non-CO₂ gas to food-system emissions, it may be that increasing non-CO₂ GHG emissions might negate China's efforts to mitigate GHG emissions⁴⁴. From the perspective of mitigation, therefore, non-CO₂ GHGs must be considered to reduce food-system GHG emissions beyond CO₂ reduction strategies. The food system itself is a primary source of anthropogenic GHGs and it will require dedicated policies to mitigate these emissions.

We analyzed the regional variations in the food-system GHG emissions among 30 provinces and eight regions based on the energy inventory and MRIO-based hybrid LCA model to examine China's food-system GHG emissions via the interregional trade network. The sources and composition of emissions varied widely in different provinces and further analysis indicated that geographical separation of production-related and consumption-related GHG emissions existed. The GHG emissions from production for provinces located in northern and western China were larger than those for wealthier central and coastal China. Owing to interregional trade, wealthy regions imported food produced in other regions, triggering the transfer of food-system GHGs. The production stage was the most important contributor to food-system GHG emissions. This means, however, that food origin regions rather than food consumption regions are responsible for large GHG emissions at the production stage. However, regional GHG emissions reduction responsibility should not be based solely on production but should also take interregional trade into account.

This study provided a broad level of life-cycle and geographical detail of national and regional food-system GHG emissions and developed a MRIO-based hybrid LCA model which was used to assess national and regional food-system GHG emissions. In contrast to previous studies, this study considered the supply chain and interregional trade network holistically rather than separately in its examination of the food-system emissions, which represents an important advance in understanding of how China's food system has developed. Furthermore, it is crucial to the prediction of China's food-system emissions in the future and to the blueprint of effective mitigation strategies aimed at preventing additional GHG emissions.

China has developed and implemented policies in recent years to reduce emissions, tackle climate change, and achieve a low-carbon, climate-resilient future. However, not enough attention has been paid to food-system. The food system contributes obviously to anthropogenic GHG emissions and is an important source of non-CO₂ gases. To meet ambitious climate-change targets, we call for specific mitigation policies for food system GHG emissions (covering both CO₂ and non-CO₂ gases). As the first step, China can set emission reduction targets for specific life cycle stages (e.g., the production stage) before establishing more general food-system mitigation targets. It is also necessary to take differences in regional food-system emissions and develop mitigation strategies and targets for each province into account. Food-system GHG emissions and food security go hand in hand.

The trade-off between food supply and climate change mitigation should be considered by policy makers. Interventions on the demand side, such as GHG certification schemes and region of origin food labelling, can also help importing regions to optimize trade and help exporting regions to generalize sustainable agricultural technologies²⁶. In light of the spillover effects of mitigation policies, a regionally strong relationship via trade networks will mandate greater interregional cooperation. Consumers are shifting to less emission-intensive foods, less food waste and more climate-friendly diets, ultimately encouraging upstream suppliers to reduce GHG emissions^{45,46}. A combination of policies and actions on both the production and consumption sides is required to fully realize the potential to reduce food-system emissions. Future studies on creating targeted policies should consider specific food commodities using more detailed models and more precise data sources. Furthermore, regional variations in diet and other consumption requirements, as well as the changing trends in interregional trade networks, also should be considered.

Method and data

System boundary. Figure 6 presents system boundary and the analytical framework of the research. The current study considered the food-system emissions in full life cycle stages (production, processing, transport, packaging, retail, consumption and waste) and estimated the emissions of four main greenhouse gases (CO₂, CH₄, N₂O and fluorinated gases (F-gases)) for the food system in nationally and in 30 Chinese provinces (excluding Tibet, Macao, Hong Kong, and Taiwan). The framework is aligned with strategies that use an integrated food-system perspective, such as the new Farm to Fork Strategy of the European Commission¹⁶.

GHGs from production that contributed to the food system were from crop cultivation and animal breeding. In this study, GHG emissions from enteric fermentation, rice cultivation, manure, synthetic fertilizers and agricultural fuel combustion are taken into account. Emissions from processing, transport, packaging and retail were mainly related to fuel combustion and refrigeration. The contribution from consumption referred to household energy use for food-related activities (e.g., refrigeration, cooking and heating food). The waste stage contained GHG from solid waste disposal and sewage treatment.

MRIO-based hybrid LCA model. We developed a MRIO-based hybrid LCA model to assess China's food-system GHG emissions. The classical MRIO model is used to describe the economic linkages accompanying the supply chain among various regions⁴⁷, with intermediate trade and final consumption. It can be expressed using the following equations:

$$X = (I - A)^{-1}F, \quad (1)$$

$$X = \begin{bmatrix} x^1 \\ x^2 \\ \vdots \\ x^n \end{bmatrix}, A = \begin{bmatrix} a^{11} & a^{12} & \dots & a^{1n} \\ a^{21} & a^{22} & \dots & a^{2n} \\ \vdots & \vdots & \ddots & \vdots \\ a^{n1} & a^{n2} & \dots & a^{nn} \end{bmatrix}, F = \begin{bmatrix} f^{11} & f^{12} & \dots & f^{1n} \\ f^{21} & f^{22} & \dots & f^{2n} \\ \vdots & \vdots & \ddots & \vdots \\ f^{n1} & f^{n2} & \dots & f^{nn} \end{bmatrix}, \quad (2)$$

where X denotes the total output vector and x_j^r is the total output of sector j located in region r , $(I - A)^{-1}$ represents the Leontief inverse matrix, F indicates the final demand matrix, I indicates the identity matrix and A is the technical coefficient matrix including submatrix $A^{rs} = (a_{ij}^{rs})$. a_{ij}^{rs} is calculated by the following equation:

$$a_{ij}^{rs} = z_{ij}^{rs} / x_j^s, \quad (3)$$

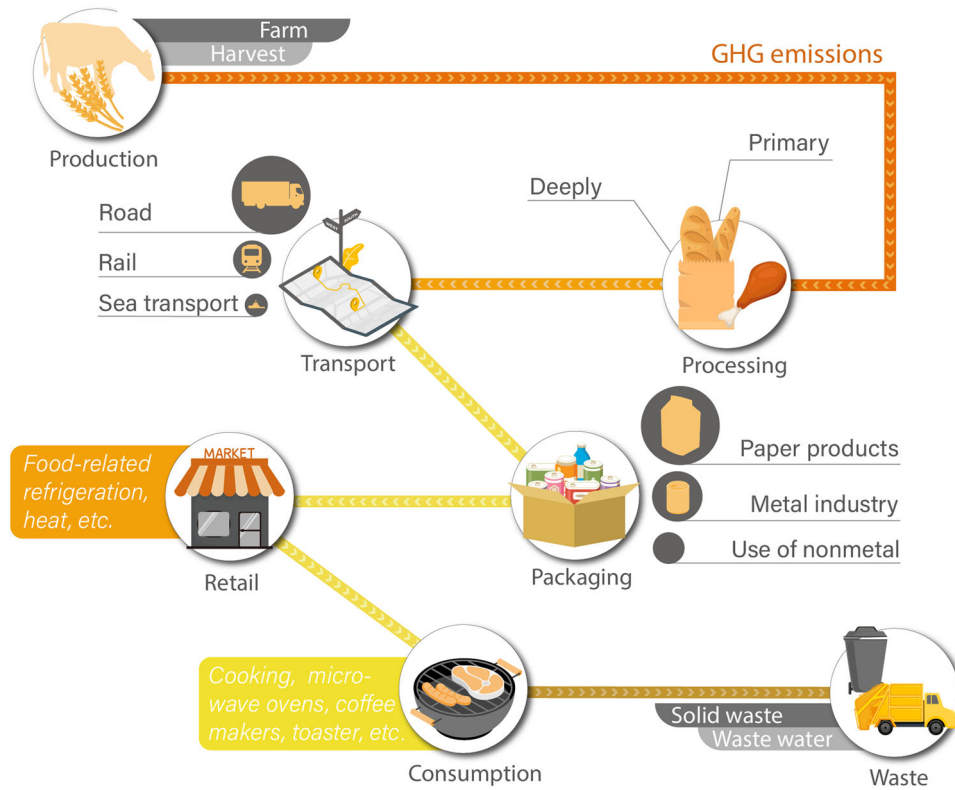


Fig. 6 System boundary. This study considers the full life cycle from cradle to grave, including production, processing, transport, packaging, retail, consumption and waste.

where z_{ij}^{rs} is the intermediate trade from sector i in region r to sector j in region s and x_j^s indicates the total output of sector j in region s .

The total input coefficient matrix B can be calculated on the basis of the technical coefficient matrix using the following equation:

$$B = (I - A)^{-1} - I. \tag{4}$$

The environmentally extended input-output model (EEIO) was developed by introducing GHG emissions from production activities on the basis of the classical MRIO model. In this study, GHG emissions is derived from section “Life cycle inventory of food-system emissions”.

Given that the contribution of the various sectors among the regions to food-system GHG emissions is diverse, we calculated the GHG emissions from food system by multiplying the sectorial food-system shares (SFSs) by the total GHG emissions of each sector. The range of the SFS was from 0 to 1. Specifically, $SFS = 1$ indicated the entire sector was attributed to the food system (e.g., agriculture), while SFSs with a value from zero to less than one showed the sectors that were partly related to the food system, such as transportation:

$$E_{k,r}^{food} = \sum_{i=1}^n E_{k,i,r} \times SFS_{i,r}, \tag{5}$$

where k indicates different types of greenhouse gas (CO_2 , CH_4 and N_2O), r denotes various regions, i represents different sectors. E is the GHG emissions and SFS indicates the sectorial emissions shares for food system. The SFSs of various sectors were in line with total input coefficient. SFSs of household consumption were from Crippa et al.¹⁶, which was closed to a household survey in China⁴⁸. Non- CO_2 GHG emissions (CH_4 , N_2O) were converted into CO_2 -eq (28 for CH_4 and 273 for N_2O), adopting the GWP100 according to the existing study³⁹.

Life cycle inventory of food-system emissions

Production. As mentioned in above sections, GHG emissions induced by non-energy activities from production included four sources: enteric fermentation, rice cultivation, manure and synthetic fertilizers. The calculation for agricultural fuel combustion, which was a part of the food-system energy emissions, is shown in section “Energy activities”. There was a difference in the types and structure of GHGs among various sources. Below, we detail the approach for calculating GHG emissions of different agricultural activities.

The CH_4 emissions of production were primarily from enteric fermentation, manure and rice cultivation. Referring to IPCC guidelines^{49,50} and Wang et al.⁵¹, the CH_4 emissions from enteric fermentation and manure were estimated by the following equation:

$$E_{FM}^{CH_4} = \sum_{p=1}^m \sum_{r=1}^n (N_{p,r}^L \times \eta_{p,r}), \tag{6}$$

where $E_{FM}^{CH_4}$ represents the CH_4 emitted from enteric fermentation or manure, $N_{p,r}^L$ denotes the livestock population of animal category p in region r and $\eta_{p,r}$ is CH_4 emissions factor for animal category p for enteric fermentation or manure management in region r .

The CH_4 emissions induced by rice cultivation were calculated by:

$$E_{RICE}^{CH_4} = \sum_{q=1}^m \sum_{r=1}^n S_{q,r}^{RICE} \times \mu_{q,r} \times t_{q,r}, \tag{7}$$

where $E_{RICE}^{CH_4}$ is the total CH_4 emitted from rice cultivation, q indicates the category of rice (e.g., early and late rice), r represents different regions, $S_{q,r}^{RICE}$ denotes the area of rice field, μ is the emission factor of rice cultivation and t represents the rice growing period.

The N₂O is released from manure and synthetic fertilizers. According to the IPCC guidelines and existing literature⁵², N₂O emissions from the production stage were estimated as:

$$E_M^{N_2O} = \sum_{p=1}^m \sum_{r=1}^n (N_{p,r}^L \times \lambda_{p,r}) + E_{Left}^{N_2O}, \quad (8)$$

where $E_M^{N_2O}$ denotes the total N₂O emitted from manure, $N_{p,r}^L$ has the same meaning as in Eq. (6), $\lambda_{p,r}$ represents the N₂O emissions factor for animal category p for manure management in region r . $E_{Left}^{N_2O}$ refers to the emissions from manure left on pasture and applied to soils. Reference to FAOSTAT (<https://www.fao.org/faostat/>), total N₂O emissions from manure left on pasture and applied to soils are 1.5 times higher than N₂O emissions from manure management.

The N₂O emissions induced by synthetic fertilizers were estimated as:

$$E_F^{N_2O} = R \times \sum_{k=1}^m \sum_{r=1}^n (NS_{k,r} + \omega \cdot NC_{k,r}) \times \sigma_{k,r} \quad (9)$$

where $E_F^{N_2O}$ is the total N₂O emitted from synthetic fertilizers, R denotes the correction factor, which is 1.571 according to a previous study⁵³, k indicates the type of crop and r represents the region. NS and NC denote the consumption of nitrogen fertilizer and compound fertilizers, respectively, ω is the share of “nitrogen” in compound fertilizer, which is set as 0.3⁵⁴, σ denotes the N₂O emissions factor.

Energy activities. Food-system energy consumption triggers GHG emissions at various stages: (1) emissions from fuel combustion in agriculture, industries, transport, households and other participants; (2) emissions induced by electricity and heat production that are used by food-system participants; (3) GHGs attributed to fuel mining, transport and leakage; and (4) indirect GHG emissions from the above stage. We estimated the GHG emissions caused by the energy activities of 42 economic sectors (in line with the MRIO table), households and disposal of waste. We consolidated the sectors in the energy inventory to remain consistent with the MRIO table and then attributed various sectors to different life cycle stages (see Supplementary Table S1).

Fossil fuel combustion. The GHG emissions from energy activities were calculated as the consumption of energy by emission factors based on the following equation:

$$E_{ENE}^i = \sum_r \sum_w C_{r,w} \times NCV_w \times EF_w \times O_w, \quad (10)$$

where E_{ENE}^i represents emissions from energy consumption for sector i , r denotes the region and w is the fuel type, C indicates the energy consumption, NCV is the net caloric value, EF refers the emission factor and O represents oxygenation efficiency. The GHG emission factors, net caloric value and oxygenation efficiency of different types of fuel (see Supplementary Table S2) were sourced from previous studies^{55,56}. We allocated the sectors in the MRIO table to the different food-system stages to estimate GHG emissions caused by energy activities at various stages (see Supplementary Table S1). The consumption of electricity and heat is converted to primary energy with reference to Shan et al.⁵⁷.

Fuel production. GHG emissions from the fuel production included CH₄ emissions from coal exploitation, and oil and natural gas systems. Coal mining and post mining both induce CH₄ emissions. Underground and surface coal mines are the two main coal exploitation methods. In comparison to surface

mining, underground mining produces obviously more CH₄ emissions per unit of coal⁴⁹.

There are large uncertainties in the calculation of CH₄ from coal mining adopting IPCC default emission factors⁵⁸. A research develops China’s province-level CH₄ emission factors from coal exploitation on the basis of data analysis of coal mining and associated discharged CH₄ emissions from 787 coal mines with various geological and operational characteristics³⁸. This dataset has a lower uncertainty than the IPCC emission factors. In order to capture GHG emissions from energy activities in the China’s food system more accurately, we applied this improved emission factor in our analysis. CH₄ emissions from coal exploitation are shown in Supplementary Table S3.

In this study, the emission factors of fugitive CH₄ from oil and natural gas systems are taken from existing literature⁵⁸, and they include venting, exploration, production and upgrading, refining/processing, storage, transport and distribution networks. Our accounting framework is consistent with the IPCC definition, and province-level active data is from China Statistical Yearbook. The average emission factor from oil systems is 2.9 kg CH₄ /m³, and the fugitive emission rates of natural gas is 1.5%.

Fluorinated gases. Fluorinated gases (F-gases) are primarily associated with the retail stage of food systems^{12,16}. The main F-gases used for refrigeration, according to IPCC guidelines, are HFC-134a, HFC-32, HFC-143, and HFC-125. To be in line with previous studies and reflect the contribution of retail stage, F-gas has also been included in our accounting framework. Unfortunately, due to a lack of detailed data, estimating F-gas emissions of China’s provincial food system is difficult. EDGAR-Food v6.0 provides national F-gases emissions at retail stage of China’s food system in 2018. We project national F-gas emissions for 2019 based on historical EDGAR-Food data adopting a linear model, which I agreed well with those published in FAOSTAT¹². We allocated the national F-gas emissions to each province based on the electricity use in the retail stage in each province, taking into account retail stage refrigeration as appliances such as refrigerators.

Waste management. Waste management is the end-of-life stage, containing solid waste management, industrial wastewater treatment and domestic sewage treatment. The primary GHG at this stage is CH₄ and CH₄ emissions from solid waste management were calculated by:

$$E_{SOL}^{CH_4} = \sum_r SW_r \times MCF_r \times DOC \times DOC_F \times FD \times 16/12, \quad (11)$$

where $E_{SOL}^{CH_4}$ represents the CH₄ emissions caused by solid waste disposal, r is the region, MCF denotes the correction coefficient of solid waste landfill following Cai et al.⁵⁹ (see Supplementary Table S4), DOC indicates the proportion of degradable organic carbon, DOC_F is the proportion of actually degradable DOC . DOC and DOC_F were set as 0.151 and 0.5, respectively, according to the literature⁵³. FD denotes the share of CH₄ in total gases escaping from solid waste disposal, which was set as 0.5 following to Du et al.⁶⁰. The conversion factor of CH₄ (CH₄/C) was 16/12.

The CH₄ emissions induced by industrial wastewater treatment were estimated as:

$$E_{WAS}^{CH_4} = \sum_r COD_r^{dis} \times WF \times MCF_{dis} + \sum_r COD_r^{re} \times WF \times MCF_{re}, \quad (12)$$

where $E_{WAS}^{CH_4}$ denotes CH₄ emissions from industrial wastewater treatment, r is the region, COD^{dis} and COD^{re} are the chemical organic demand for wastewater directly discharged and cleaned

up by wastewater treatment facilities, respectively. WF represents the emission coefficient that took a value of 0.25 from the IPCC guidelines^{49,50}, MCF_{dis} and MCF_{re} denote correction coefficients of COD^{dis} and COD^{re} , respectively, which were 0.458⁵³ and 0.1^{49,50}.

The CH_4 emissions caused by domestic sewage treatment were calculated based on the following equation:

$$E_{SEW}^{CH_4} = \sum_r BOD_r^{dis} \times SF \times MCF_{dis} + \sum_r BOD_r^{re} \times SF \times MCF_{re}, \quad (13)$$

where $E_{SEW}^{CH_4}$ is the total CH_4 emitted from domestic sewage treatment, r represents the region, BOD^{dis} and BOD^{re} indicate the biological oxygen demand for wastewater directly discharged and cleaned up by wastewater treatment facilities, respectively, SF denotes the emission coefficient, which takes a value of 0.6 following the IPCC guideline, MCF_{dis} and MCF_{re} denote the correction coefficients of BOD^{dis} and BOD^{re} , respectively, which were 0.1⁵³ and 0.165^{49,50}.

CH_4 and N_2O from domestic wastewater are estimated by a recent investigation conducted by Wang et al.³⁹ in a recent study. The dataset includes provincial detailed GHG emissions from domestic wastewater based on wastewater treatment plants and other facilities in China, considering biological treatment processes and discharge pathways.

Data sources and compilation. This study adopted data from four categories: agricultural statistics, the MRIO table, the energy and the waste inventory. Agricultural statistics were used to estimate the emissions generated at the production stage of the food system. We obtained China's provincial agricultural statistics in 2019 from China Agriculture Yearbook⁶¹, including provincial inventories of livestock by category, the usage of nitrogen and compound fertilizers, all types of crop acreage and yields and the rice areas with different varieties (early, middle and late) by province. The corresponding emission factors can be found in Supplementary Table S6-S10.

The MRIO table was obtained from Carbon Emission Account and Datasets (CEADs)⁶². The 2012–2017 MRIO table quantified the intermediate trade and final consumption covering 42 sectors in 30 of China's provinces (in line with this study) based on the gravity model. The MRIO tables compiled by CEADs are recognized as a comprehensive and reliable data source. The 2019 MRIO table was missing because the data are released every 5 years. Because the MRIO table was used to estimate input coefficients and trade structure in our study, we adopted the 2017 MRIO table. The current study excluded the influence of international trade and technology homogeneities because we focused on food-system GHG emissions across China.

The provincial energy inventory in 2019 was constructed by CEADs, covering 20 types of energy and 30 provinces in China^{57,63–65}. The provincial inventory of solid waste disposal was derived from the China Urban Construction Statistical Yearbook⁶⁶. The provincial inventory of industrial wastewater treatment and chemical oxygen demand removed were from the China Environmental Statistical Yearbook⁶⁷.

Uncertainty analysis. The uncertainty in our estimation of food system emissions mainly stems from the emission factors and activity data adopted. Previous studies assigned different uncertainty to various food system emission sources, and the similar approach is employed in this study. GHG emissions induced by non-energy activities from production are accounted based on IPCC guidelines⁴⁹, and the range is 30–70% across various activities. FAOSTAT assigned uncertainties of 50% and 30%

respectively to land-based change and farm-gate processes of global inventory¹². Given the applicability of IPCC emission factors to China, we assign 40% of the uncertainties to components of non-energy activities from production. Emissions from the energy activities are calculated based on previous works^{38,56–58}. We therefore attribute an overall uncertainty of 30% to energy activities. The accounting of F-gas emissions is on the basis of the work of Crippa et al.¹⁶, and thus has a 46% uncertainty with reference to their work. GHG emissions from solid waste are assigned a 30% uncertainty, which is consistent with the work of Tubiello et al.¹². The estimate of GHG emissions from wastewater treatment refers to previous literature³⁹. And uncertainties of wastewater treatment are from this work, with 60%, 150%, and 4% uncertainties for CH_4 , N_2O , and CO_2 , respectively. Moreover, all uncertainties can be combined adopting the Eqs. (14)–(15), which is suggested by IPCC guideline. The Eq. (14) is applicable to the merger among related GHG sources, and the Eq. (15) applies to the merger among unrelated sources.

$$U_{total} = \frac{\sqrt{(U_1 \bullet x_1)^2 + (U_2 \bullet x_2)^2 + \dots + (U_3 \bullet x_3)^2}}{|x_1 + x_2 + \dots + x_n|} \quad (14)$$

$$U_{total} = \sqrt{(U_1)^2 + (U_2)^2 + \dots + (U_n)^2} \quad (15)$$

Where U_{total} indicates total uncertainty on the basis of 95% confidence interval, U_i is uncertainty of emission source i , and x_i refers to the uncertain emissions.

Data availability

The data that support the findings of this study and Supplementary Table 2, 3, 4, 6, 7, 8, 9 and 10 are archived at <https://doi.org/10.6084/m9.figshare.22083959>. Raw data are available from the following sources. Energy inventories, GHG emission inventory and the 2017 China MRIO table can be sourced from the China Emission Accounts and Datasets (<http://www.ceads.net/>). China's provincial agricultural statistics in 2019 from China Agriculture Yearbook (<https://data.cnki.net/yearBook/single?id=N2022030154>). The provincial inventory of solid waste disposal was derived from the China Urban Construction Statistical Yearbook (<https://data.cnki.net/yearBook/single?id=N2021110027>). The provincial inventory of industrial wastewater treatment and chemical oxygen demand removed were from the China Environmental Statistical Yearbook (<https://data.cnki.net/yearBook/single?id=N2021070128>).

Code availability

The code to process and analyse the primary data collected in this study will be made available upon request.

Received: 5 December 2022; Accepted: 17 April 2023;

Published online: 09 May 2023

References

- IPCC. Climate Change 2022: Impacts, Adaptation and Vulnerability. Contribution of Working Group II to the Sixth Assessment Report of the Intergovernmental Panel on Climate Change. (Cambridge University Press, 2022).
- Weyant, J. R., de la Chesnaye, F. C. & Blanford, G. J. Overview of EMF-21: Multigas mitigation and climate policy. *Energy J* **27**, 1–32 (2006).
- Shindell, D. et al. Simultaneously mitigating near-term climate change and improving human health and food security. *Science* **335**, 183–189 (2012).
- Su, X. et al. Emission pathways to achieve 2.0 °C and 1.5 °C climate targets. *Earth Future* **5**, 592–604 (2017).
- Ou, Y. et al. Deep mitigation of CO_2 and non- CO_2 greenhouse gases toward 1.5 °C and 2 °C futures. *Nat. Commun.* **12**, 6245 (2021).
- Frank, S. et al. Agricultural non- CO_2 emission reduction potential in the context of the 1.5 °C target. *Nat. Clim. Chang.* **9**, 66–+ (2019).
- Burke, M., Davis, W. M. & Diffenbaugh, N. S. Large potential reduction in economic damages under UN mitigation targets. *Nature* **557**, 549–+ (2018).

8. Poore, J. & Nemecek, T. Reducing food's environmental impacts through producers and consumers. *Science* **360**, 987–992 (2018).
9. Fanzo, J. et al. Viewpoint: rigorous monitoring is necessary to guide food system transformation in the countdown to the 2030 global goals. *Food Policy* **104**, 102163 (2021).
10. Rosenzweig, C. et al. Climate change responses benefit from a global food system approach. *Nat. Food* **1**, 94–97 (2020).
11. Leip, A., Bodirsky, B. L. & Kugelberg, S. The role of nitrogen in achieving sustainable food systems for healthy diets. *Glob. Food Secur.-Agric.Policy* **28**, 100408 (2021).
12. Tubiello, F. N. et al. Pre- and post-production processes increasingly dominate greenhouse gas emissions from agri-food systems. *Earth Syst. Sci. Data* **14**, 1795–1809 (2022).
13. FAO. Greenhouse gas emissions from agrifood systems. Global, regional and country trends, 2000–2020. <https://www.fao.org/3/cc2672en/cc2672en.pdf> (2022).
14. Carlson, K. M. et al. Greenhouse gas emissions intensity of global croplands. *Nat. Clim. Change* **7**, 63–68 (2017).
15. Tubiello, F. N. et al. Greenhouse gas emissions from food systems: building the evidence base. *Environ. Res. Lett.* **16**, 065007 (2021).
16. Crippa, M. et al. Food systems are responsible for a third of global anthropogenic GHG emissions. *Nat. Food* **2**, 198–209 (2021).
17. Li, T., Baležentis, T., Makutėnienė, D., Streimikiene, D. & Kriščiukaitienė, I. Energy-related CO₂ emission in European Union agriculture: driving forces and possibilities for reduction. *Appl. Energy* **180**, 682–694 (2016).
18. Lin, B. & Xu, B. Factors affecting CO₂ emissions in China's agriculture sector: a quantile regression. *Renew. Sust. Energy Rev.* **94**, 15–27 (2018).
19. Waheed, R., Chang, D., Sarwar, S. & Chen, W. Forest, agriculture, renewable energy, and CO₂ emission. *J. Clean Prod.* **172**, 4231–4238 (2018).
20. Burney, J. A., Davis, S. J. & Lobell, D. B. Greenhouse gas mitigation by agricultural intensification. *Proc. Natl Acad. Sci. USA* **107**, 12052–12057 (2010).
21. Bajželj, B. et al. Importance of food-demand management for climate mitigation. *Nat. Clim. Change* **4**, 924–929 (2014).
22. Garnier, J. et al. Long-term changes in greenhouse gas emissions from French agriculture and livestock (1852–2014): From traditional agriculture to conventional intensive systems. *Sci. Total Environ.* **660**, 1486–1501 (2019).
23. Tubiello, F. N. et al. Methods for estimating greenhouse gas emissions from food systems. Part III: energy use in fertilizer manufacturing, food processing, packaging, retail and household consumption. <https://doi.org/10.4060/cb7473en>.
24. Rosenzweig, C., Tubiello, F. N., Sandalow, D., Benoit, P. & Hayek, M. N. Finding and fixing food system emissions: the double helix of science and policy. *Environ. Res. Lett.* **16**, 061002 (2021).
25. Ziegler, F., Tyedmers, P. H. & Parker, R. W. R. Methods matter: improved practices for environmental evaluation of dietary patterns. *Glob. Environ. Change-Human Policy Dimens* **73**, 102482 (2022).
26. Zhao, X. et al. Linking agricultural GHG emissions to global trade network. *Earth's Future* **8**, e2019EF001361 (2020).
27. Foong, A., Pradhan, P., Frör, O. & Kropp, J. P. Adjusting agricultural emissions for trade matters for climate change mitigation. *Nat Commun* **13**, 3024 (2022).
28. Hong, C. et al. Land-use emissions embodied in international trade. *Science* **376**, 597–603 (2022).
29. Roy, P. et al. A review of life cycle assessment (LCA) on some food products. *J. Food Eng.* **90**, 1–10 (2009).
30. Heller, M. C., Keoleian, G. A. & Willett, W. C. Toward a life cycle-based, diet-level framework for food environmental impact and nutritional quality assessment: a critical review. *Environ. Sci. Technol.* **47**, 12632–12647 (2013).
31. Ladha-Sabur, A., Bakalis, S., Fryer, P. J. & Lopez-Quiroga, E. Mapping energy consumption in food manufacturing. *Trends Food Sci. Technol.* **86**, 270–280 (2019).
32. Chen, G. Q. & Han, M. Y. Global supply chain of arable land use: production-based and consumption-based trade imbalance. *Land Use Policy* **49**, 118–130 (2015).
33. Xia, Y. & Yan, B. Energy-food nexus scarcity risk and the synergic impact of climate policy: a global production network perspective. *Environ. Sci. Policy* **135**, 26–35 (2022).
34. Crippa, M. et al. High resolution temporal profiles in the emissions database for global atmospheric research. *Sci. Data* **7**, 121 (2020).
35. Gong, S. & Shi, Y. Evaluation of comprehensive monthly-gridded methane emissions from natural and anthropogenic sources in China. *Sci. Total Environ.* **784**, 147116 (2021).
36. Zhang, F., Jin, G. & Liu, G. Evaluation of virtual water trade in the Yellow River Delta, China. *Sci. Total Environ.* **784**, 147285 (2021).
37. Zhao, X. et al. Physical and virtual water transfers for regional water stress alleviation in China. *Proc. Natl Acad. Sci. USA* **112**, 1031–1035 (2015).
38. Zhu, T., Bian, W., Zhang, S., Di, P. & Nie, B. An improved approach to estimate methane emissions from coal mining in China. *Environ. Sci. Technol.* **51**, 12072–12080 (2017).
39. Wang, D. et al. Greenhouse gas emissions from municipal wastewater treatment facilities in China from 2006 to 2019. *Sci Data* **9**, 317 (2022).
40. Nayak, D. et al. Management opportunities to mitigate greenhouse gas emissions from Chinese agriculture. *Agric. Ecosyst. Environ.* **209**, 108–124 (2015).
41. Dong, Y. & Miller, S. A. Assessing the lifecycle greenhouse gas (GHG) emissions of perishable food products delivered by the cold chain in China. *J. Cleaner Prod.* **303**, 126982 (2021).
42. Han, J. et al. A critical assessment of provincial-level variation in agricultural GHG emissions in China. *J. Environ. Manag.* **296**, 113190 (2021).
43. Zhang, H., Xu, Y. & Lahr, M. L. The greenhouse gas footprints of China's food production and consumption (1987–2017). *J. Environ. Manag.* **301**, 113934 (2022).
44. Zhang, B., Zhang, Y., Zhao, X. & Meng, J. Non-CO₂ greenhouse gas emissions in China 2012: inventory and supply chain analysis. *Earth's Future* **6**, 103–116 (2018).
45. Xiong, X. et al. How urbanization and ecological conditions affect urban diet-linked GHG emissions: new evidence from China. *Resour. Conserv. Recycling* **176**, 105903 (2022).
46. Yue, Q., Xu, X., Hillier, J., Cheng, K. & Pan, G. Mitigating greenhouse gas emissions in agriculture: from farm production to food consumption. *J. Cleaner Prod.* **149**, 1011–1019 (2017).
47. Liu, G. & Zhang, F. China's carbon inequality of households: perspectives of the aging society and urban-rural gaps. *Resour. Conserv. Recycling* **185**, 106449 (2022).
48. Zheng, X. et al. Characteristics of residential energy consumption in China: findings from a household survey. *Energy Policy* **75**, 126–135 (2014).
49. IPCC. 2006 IPCC Guidelines for National Greenhouse Gas Inventories. (2006).
50. IPCC. 2019 Refinement to the 2006 IPCC Guidelines for National Greenhouse Gas Inventories. (2019).
51. Wang, K., Zhang, J., Cai, B. & Liang, S. Estimation of Chinese city-level anthropogenic methane emissions in 2015. *Resources, Conservation and Recycling* **175**, 105861 (2021).
52. Zhou, F. et al. A New High-Resolution N₂O Emission Inventory for China in 2008. *Environ. Sci. Technol.* **48**, 8538–8547 (2014).
53. Yuan, R. & Wang, J. Impacts of poverty alleviation on household GHG footprints in China. *Energy Economics* **103**, 105602 (2021).
54. Zhuang, M. et al. Emissions of non-CO₂ greenhouse gases from livestock in China during 2000–2015: Magnitude, trends and spatiotemporal patterns. *J. Environ. Manag.* **242**, 40–45 (2019).
55. Liu, Z., Geng, Y., Lindner, S. & Guan, D. Uncovering China's greenhouse gas emission from regional and sectoral perspectives. *Energy* **45**, 1059–1068 (2012).
56. Liu, Z. et al. Reduced carbon emission estimates from fossil fuel combustion and cement production in China. *Nature* **524**, 335–338 (2015).
57. Shan, Y., Huang, Q., Guan, D. & Hubacek, K. China CO₂ emission accounts 2016–2017. *Sci Data* **7**, 54 (2020).
58. Peng, S. et al. Inventory of anthropogenic methane emissions in mainland China from 1980 to 2010. *Atmosph. Chem. Phys.* **16**, 14545–14562 (2016).
59. Cai, B. et al. Estimation of methane emissions from municipal solid waste landfills in China based on point emission sources. *Adv. Climate Change Research* **5**, 81–91 (2014).
60. Du, M. et al. Quantification of methane emissions from municipal solid waste landfills in China during the past decade. *Renew. Sustain. Energy Rev.* **78**, 272–279 (2017).
61. DREB. China Agriculture Yearbook. (China Statistics Press, 2020).
62. Zheng, H. et al. Regional determinants of China's consumption-based emissions in the economic transition. *Environ. Res. Lett.* **15**, 074001 (2020).
63. Shan, Y. et al. China CO₂ emission accounts 1997–2015. *Scientific Data* **5**, 170201 (2018).
64. Shan, Y. et al. New provincial CO₂ emission inventories in China based on apparent energy consumption data and updated emission factors. *Applied Energy* **184**, 742–750 (2016).
65. Guan, Y. et al. Assessment to China's recent emission pattern shifts. *Earth's Future* **9**, e2021EF002241 (2021).
66. MOHURD. China Urban and Rural Construction Statistical Yearbook. (China Planning Press, 2020).
67. NBS & MEE. China Environmental Statistical Yearbook. (China Statistics Press, 2020).

Acknowledgements

This research was financially supported by National Natural Science Foundation of China (Grant No. 72221002) and Strategic Priority Research Program of the Chinese Academy of Sciences (Grant No. XDA23070400).

Author contributions

G.L.: Methodology, Software, Writing—original draft, Data curation. F.Z.: Data curation, Conceptualization, Writing—review & editing. X.D.: Supervision, Writing—review & editing, funding acquisition.

Competing interests

The authors declare no competing interests.

Additional information

Supplementary information The online version contains supplementary material available at <https://doi.org/10.1038/s43247-023-00809-2>.

Correspondence and requests for materials should be addressed to Xiangzheng Deng.

Peer review information *Communications Earth & Environment* thanks the anonymous reviewers for their contribution to the peer review of this work. Primary Handling Editor: Aliénor Lavergne. Peer reviewer reports are available.

Reprints and permission information is available at <http://www.nature.com/reprints>

Publisher's note Springer Nature remains neutral with regard to jurisdictional claims in published maps and institutional affiliations.



Open Access This article is licensed under a Creative Commons Attribution 4.0 International License, which permits use, sharing, adaptation, distribution and reproduction in any medium or format, as long as you give appropriate credit to the original author(s) and the source, provide a link to the Creative Commons license, and indicate if changes were made. The images or other third party material in this article are included in the article's Creative Commons license, unless indicated otherwise in a credit line to the material. If material is not included in the article's Creative Commons license and your intended use is not permitted by statutory regulation or exceeds the permitted use, you will need to obtain permission directly from the copyright holder. To view a copy of this license, visit <http://creativecommons.org/licenses/by/4.0/>.

© The Author(s) 2023